Phase Dependence of Microwave-Assisted Switching of a Single Magnetic Nanoparticle

R. Piquerel, O. Gaier, E. Bonet, C. Thirion, and W. Wernsdorfer
Institut Néel, 25 rue des Martyrs, F-38042 Grenoble, Cedex 9, France
(Received 8 May 2013; published 19 March 2014)

Microwave-assisted switching of the magnetization is an efficient way to reduce the magnetic field required to reverse the magnetization of nanostructures. Here, the phase sensitivity of microwave-assisted switching of an individual cobalt nanoparticle is studied using a pump-probe technique. The pump microwave pulse prepares an initial state of the magnetization, and the probe pulse tests its stability against switching. Precession states are established, which are stable against switching. Their basin of attraction is measured and is in qualitative agreement with numerical macrospin calculations. The damping parameter is evaluated using the variable delay pump-probe technique.

DOI: 10.1103/PhysRevLett.112.117203 PACS numbers: 75.60.Jk, 75.50.Tt, 75.75.Jn, 84.40.-x

Microwave-assisted switching (MAS) of the magnetization is an efficient way to reduce the static magnetic field required to reverse the magnetization of small patterned ferromagnets or nanoparticles. The pioneer work performed on an individual magnetic nanoparticle [1] has been followed by experimental studies, which demonstrate the efficiency of MAS on assemblies of magnetic elements [2], patterned elements [3–6] and nanoparticles [7], and the oscillations of domain walls excited by current pulses [8]. Theoretical studies have focused mainly on optimizing the switching scenario, often under the assumption of uniaxial symmetry. They addressed the phase dependence for very long microwave pulses [9–13] and investigated the influence of the polarization [14], the frequency modulation [15–17] and a full waveform optimization [18], as well as the temperature [19,20].

We provide here numerical and experimental evidence of a strong microwave phase effect, considering the situation where magnetization reversal is achieved in an individual nanoparticle by the combination of a static magnetic field, at a fixed angle from the easy axis, and a microwave pulse. The dc field creates a shallow metastable energy well in the energy landscape of the magnetization, a deeper well close to the direction of the dc field, and a saddle point in between the two energy wells. The magnetization is initially prepared in the metastable well, and a short rf field pulse is used to switch the magnetization to the other well.

We show that the rf pulse may fail to reverse the magnetization if it has the wrong phase, even if the pulse is very long and has more than sufficient amplitude. When this happens, the pulse drives the magnetization into a stable precession state inside the metastable well. If the pulse is long enough for the transient dynamics to be damped away, then this motion becomes a periodic motion with the same period as the driving rf field. These precession states are very stable against perturbations and have to be avoided when MAS is applied to magnetic elements.

Before presenting the experimental part, it is helpful to perform numerical simulations to visualize these stable precession states and to study the role of the phase in the magnetization dynamics. We used a macrospin model with uniaxial anisotropy along the z axis, a static field in the yz plane, and a rf field pulse linearly polarized along x. The energy density is

$$E/V = -Km_z^2 - \mu_0 M_s \mathbf{m} \cdot (\mathbf{H}_{\mathrm{dc}} + \mathbf{H}_{\mathrm{ac}}), \tag{1}$$

where V is the volume of the particle, K the anisotropy constant, m_z is the z component of reduced magnetization $\mathbf{m} = \mathbf{M}/M_s$, M_s is the modulus of the magnetization, $\mathbf{H}_{\mathrm{dc}}$ is the static applied field, and $\mathbf{H}_{\mathrm{ac}}$ is a monochromatic rf field. The trajectory of $\mathbf{m}$ in the energy landscape E is obtained by numerically integrating the Landau-Lifshitz-Gilbert (LLG) equation

$$\frac{d\mathbf{m}}{dt} = -\gamma_0 \mathbf{m} \times \mathbf{H}_{\mathrm{eff}} + \alpha\left(\mathbf{m} \times \frac{d\mathbf{m}}{dt}\right), \tag{2}$$

where $\mathbf{H}_{\mathrm{eff}} = -\frac{1}{\mu_0 M_s V}\frac{\partial E}{\partial \mathbf{m}}$ is the effective field. We used the following parameters: the anisotropy field is 300 mT, similar to the experimental value, the static field is $\mu_0 \mathbf{H}_{\mathrm{dc}} = (0, 30, -150)$ mT, in Cartesian coordinates, $\gamma_0/\mu_0 = 176.086\ \mathrm{ns}^{-1}\,\mathrm{T}^{-1}$, and $\alpha = 0.005$. With these parameters, the energy landscape has a metastable minimum at $\mathbf{m} = (0, 0.204, 0.979)$ in Cartesian coordinates, a saddle point S at (0,0.822,0.569), and a global minimum at (0,0.067,−0.998). The initial magnetization state is in the metastable well. When applying the rf field, the magnetization either switches towards the global minimum or gets "trapped" in a precessional motion inside the metastable well. We integrated the LLG equation until the magnetization reached a steady state. When the magnetization did not switch, a stable precession state was reached after typically 20 ns.

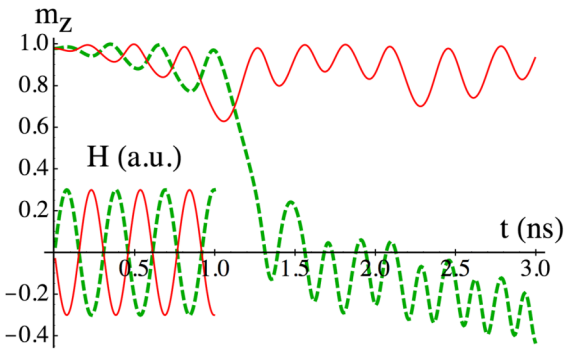

FIG. 1 (color online). Computed time dependence of the m_z component of the magnetization under an applied rf field for a successful (dashed green) and unsuccessful (continuous red) reversal. Bottom-left: time dependence of the two corresponding rf fields having the same amplitude $A = 7.51$ mT and a different phase. For clarity, only the first nanosecond is plotted.

Figure 1 displays examples of successful and unsuccessful MAS. The two scenarios differ only in the initial phase of the rf pulse. In one scenario (dashed green trajectory), the rf field succeeds to reverse the magnetization, while in the other scenario (red trajectory), the magnetization gets trapped in a precessional motion inside the metastable well. The inset of Fig. 1 shows the time dependence of the rf field for both scenarios using the corresponding colors. Figure 2 shows the same trajectory in a more detailed view around the metastable well using a transverse Mercator projection [21] onto the static energy landscape. The green trajectory gets out of the metastable energy well quite fast (about three precessions), while the red trajectory slowly converges to a periodic precession. This periodic motion acts as a "trap" that prevents reversal.

The most surprising feature of this simulation is the fact that, although the stable orbit acts like a trap for the magnetization, the successful reversal trajectory manages to cross this orbit without getting trapped. This is an effect of the relative phase of the magnetization motion relative to the rf field. Although the successful MAS trajectory crosses the stable orbit, it does so at a different phase of the rf field compared to the stable precessional motion. We conclude that the phase of the periodic precession relative to the rf field is a very important feature of this periodic motion. In fact, during the stable precessional motion, the relative phase is such that there is almost no energy transferred from the rf field to the magnetization.

Let us now fix the initial phase of the rf field and vary the initial state of the magnetization. Figure 3 shows a map of the initial states that lead to either reversal or no reversal. The complex black shape with many ramifications is the set of initial conditions that lead to the stable precession in the metastable energy well. It is known as the basin of attraction of this precessional motion. The gray fingers in between the ramifications of the basin of attraction are initial states that lead to magnetization reversal. The simulations of many trajectories led us to the following observations: If the initial state is inside one of the gray fingers, the magnetization precesses a few turns inside the metastable well before reversal. Between adjacent fingers, there is exactly one extra turn of precession inside the metastable well. For initial states at the tips of the fingers, the magnetization gets "stuck" at about the saddle point and then falls back on the metastable well. At the complex borders of the fingers, more complex trajectories are observed, suggesting the presence of chaos [22].

In order to provide experimental evidence of the influence of an initial magnetization state, we developed a specific pump-probe experiment using a microSQUID setup [23]. We performed MAS experiments on a single 20 nm Co nanoparticle embedded in amorphous carbon at

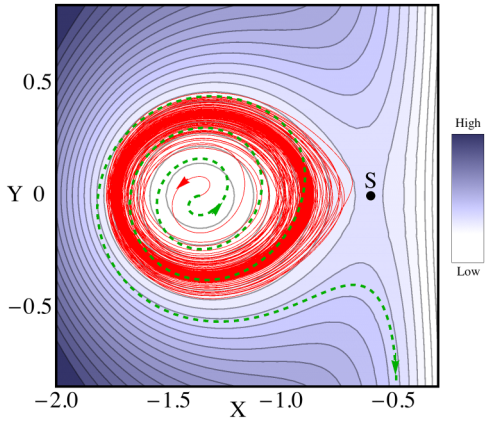

FIG. 2 (color online). Two different magnetization trajectories projected onto the static energy landscape E and its isoenergy curves. X and Y are defined by the Mercator projection. Successful (dashed green) and unsuccessful (continuous red) reversals are compared. S is the saddle point of E.

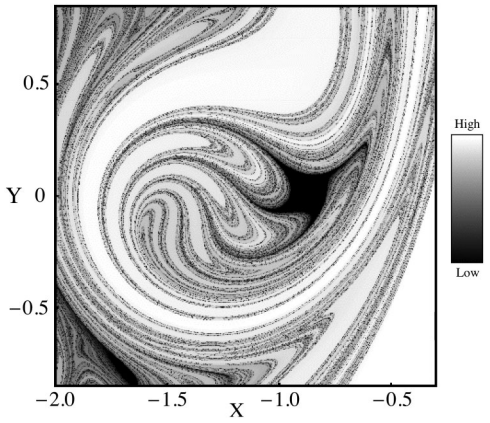

FIG. 3. MAS as a function of the initial state inside the metastable energy well (Fig. 2). Black regions are the initial states that lead to a precessional motion inside this well, preventing reversal. Gray regions are those initial states that lead to reversal. Darker initial states take longer to reverse.

40 mK. The energy barrier for reversal (approximately 6600 K) being 5 orders of magnitude larger than the temperature thermal effects can safely be ignored. We used a similar experimental setup as in Ref. [1] but it was equipped with an ultrawideband arbitrary waveform generator allowing the generation of phase-controlled rf fields. The general idea of this pump-probe experiment is to prepare the magnetization state with the pump pulse and to investigate the dynamical properties of that state with the probe pulse.

There are several parameters that control the full shape of the rf field sequence: the amplitude, phase and duration of the pump and probe pulse (A_0, ϕ_0, τ_0) and (A_1, ϕ_1, τ_1), respectively, and the frequency of the pump and probe pulse is fixed to the same value f. The rise time and fall time of each pulse is fixed to about 0.2 ns. The delay ΔT between the pump and probe is used to let the magnetization precess freely.

A_0 controls how far the magnetization gets from the local energy minimum. The phase ϕ_0 sets the phase of the precession, i.e., the direction of the initial state relative to the local energy minimum. The pump pulse duration $\tau_0 = 3.5$ ns is chosen to be too short to achieve reversal, even at the maximum amplitude A_0. The probe pulse duration $\tau_1 = 20$ ns, the phase $\phi_1 = 0$, and amplitude A_1 are fixed and chosen to switch the magnetization starting from the equilibrium state in the metastable well. By varying the parameters of the pump pulse (A_0, ϕ_0), we study the MAS as a function of the initial magnetization, just like in the previous numerical study. Increasing both parameters continuously (A_0, ϕ_0) allows the magnetization to reach any initial starting condition.

Figure 4 presents both map measurements (left column) and numerical simulations using the exact same protocol as in the measurements (right column). From top to bottom the delay ΔT between the pump and probe pulse was varied: 0, 0.294, and 2.94 ns corresponding to, respectively, 0, 1, and 10 precessions. Another comparison between experiment and calculation for 0.368 ns corresponding to one precession and a quarter is given in Ref. [24]. Each map $\mathcal{M}$ shows large black nonswitching and switching regions interpenetrating each other. In the black nonswitching regions, the pump pulse sets an initial magnetization state, where the magnetization is dynamically trapped. If the magnetization were started from the metastable equilibrium state, it would have switched with the probe pulse. However, in the black regions, the magnetization cannot escape from the metastable well, that is, the black regions correspond to the pump parameters that lead to nonswitching trajectories of the magnetization, such as the red curve in Fig.2. These black regions of nonswitching are qualitatively similar to Fig.3, even though the switching in Fig. 4 is plotted as a function of the pump parameters. This black region of nonswitching is qualitatively similar to Fig. 3, even though the switching in Fig. 4 is plotted as a function of the pump parameters. The

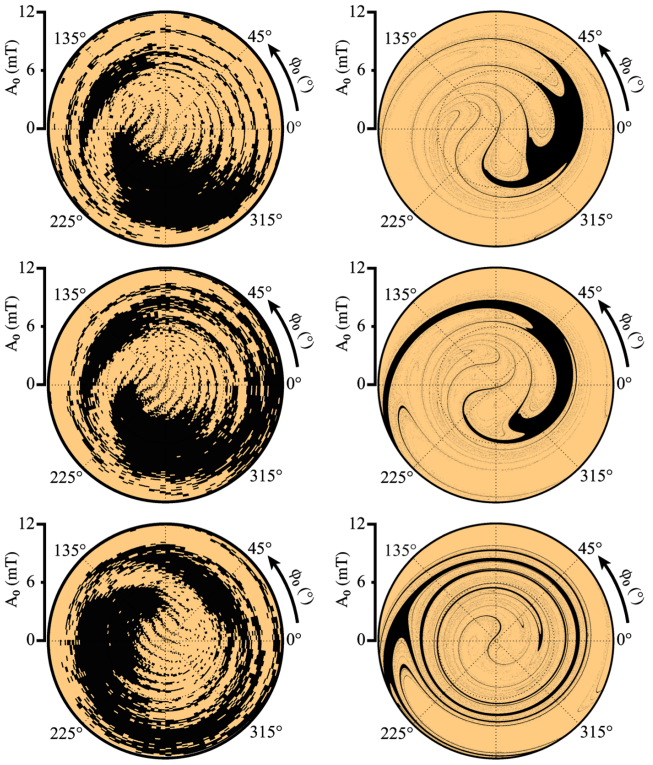

FIG. 4 (color online). Switching state maps for different delays. Switching and nonswitching regions are evidenced by the pump-probe technique. In each map, the switching is measured as a function of the phase and amplitude of the pump pulse displayed here in polar coordinates. Black means no switching, orange regions do switch. On the left are the experimental data obtained on a 20 nm nanoparticle for different delays (top to bottom) 0, 1, and 10 precessions. Additional data are presented in Ref. [24]. On the right are the numerical simulations following the experimental protocol with the same delays.

effect of increasing the delay ΔT is qualitatively simple. After the preparation by the pump rf field, the magnetization precesses freely during that duration ΔT. Then the probe rf field reverses or does not reverse the magnetization. The phase sensitivity evidenced in numerical calculations and experiments comes from the fact that the phase either suits or does not suit the magnetization. Another important parameter is the exact position where the magnetization has settled after its relaxation. It can be either on the good side of the potential well, close to the saddle point, enabling the switching of the magnetization, or on the other side, making the switching unlikely.

There is a certain correspondence between Figs. 3 and 4; that is, the pump rf field prepares a magnetization state, and the probe signal allows us to check the possibility of switching. The differences are due to the nonlinearities of the system complicating the mapping from pump parameters to initial magnetization. If the delay ΔT is not an integer, it will end in a global rotation of the whole map, as shown in Ref. [24]. The angle of precession near the center of the figure is a few degrees, which means that the free

small-angle precession frequency near the local energy minimum is slightly above our rf pulse frequency of 3.4 GHz. This is consistent with the fact that we have chosen a static dc field and a rf frequency that make MAS possible at moderate rf amplitudes. Higher amplitudes are required when the applied frequency differs significantly from this optimum, which is dependent on the curvature of the energy landscape and, thus, on the dc field. Upon closer examination, some differences in the shape of experimental and theoretical maps in Fig. 4 can be seen. They are mainly the consequence of the nonharmonicities of the energy well that make the precession frequency energy dependent. This depends on the static energy density, which was kept uniaxial here to simplify the problem, without any qualitative change in the result. We tested both a biaxial and a small cubic magnetocrystalline anisotropy term and found that it does not change the global features of the maps $\mathcal{M}$.

We measured different maps $\mathcal{M}$ as a function of the delay ΔT to investigate the damping parameter α during free relaxation of the magnetization. While most experiments such as ferromagnetic resonance or Brillouin light scattering can be used to estimate the damping parameter under some excitations of the magnetization, here we probe the effect of the damping without any external signal, that is, the "free" damping. The free precession induces a rotation of the map proportional to ΔT. For $\alpha = 0$, $\mathcal{M}(\Delta T)$ is invariant for any delay ΔT corresponding to an exact integer number of precessions. For $\alpha \neq 0$, the magnetization relaxes during ΔT, resulting after a turn of precession in a slightly modified magnetization state, which is deeper in the energy well. In the first approximation, assuming that in the center of the maps the potential is harmonic, the logarithmic change of the precessional amplitude is proportional to $\alpha\Delta T$. Thus, precession and damping combine into a simple shift of the map in $(\log A_0, \phi_0)$ coordinates. Using these coordinates, we computed the correlations between $\mathcal{M}(\Delta T = 0)$ and $\mathcal{M}(\Delta T)$ as a function of the delay ΔT using only the small-amplitude part of the maps. A linear fit of the shift in $\log A_0$ versus the delay yields an estimate of $\alpha = 0.005$. This approximation is not valid for long delays of above 10 ns where nonlinearities become dominant and the map becomes distorted.

In conclusion, we investigated the influence of the relative phase between a microwave field excitation and the magnetization of an individual cobalt nanoparticle. This phase effect was established through numerical simulations of a macrospin using the LLG equation showing that stable nonswitching trajectories exist for certain relative phases. Using a pump-probe technique, we found that the magnetization can reach a dynamic state where it is trapped, even when applying a rf field that would have switched the magnetization starting from the equilibrium in the metastable energy well. We measured and simulated these nonswitching dynamical states of the magnetization and their basin of attraction. The free precession of the magnetization was studied using a delay time between the pump and probe pulse. Applying the correlation technique on the switching maps allowed the estimation of the damping parameter of free magnetization precession. We found a value of $\alpha = 0.005$, which is compatible with the numerical simulations. Thus, for future applications of the MAS technique to read or write information on small ferromagnets, one should carefully control the phase; otherwise, the magnetization can be trapped in a nonswitching trajectory unless increasing the microwave power significantly.

We acknowledge the cluster "Microélectronique Nanosciences et Nanotechnologies," the ANR Foundation for Project No. ANR-08-NANO-039-01, and CIBLE for the Ph.D. thesis funding.

[1] C. Thirion, W. Wernsdorfer, and D. Mailly, Nat. Mater. **2**, 524 (2003).
[2] H. T. Nembach, H. Bauer, J. M. Shaw, M. L. Schneider, and T. J. Silva, Appl. Phys. Lett. **95**, 062506 (2009).
[3] G. Woltersdorf and C. H. Back, Phys. Rev. Lett. **99**, 227207 (2007).
[4] Y. Nozaki, M. Ohta, S. Taharazako, K. Tateishi, S. Yoshimura, and K. Matsuyama, Appl. Phys. Lett. **91**, 082510 (2007).
[5] T. Moriyama, R. Cao, J. Q. Xiao, J. Lu, X. R. Wang, Q. Wen, and H. W. Zhang, J. Appl. Phys. **103**, 07A906 (2008).
[6] M. Laval, J. J. Bonnefois, J. F. Bobo, F. Issac, and F. Boust, J. Appl. Phys. **105**, 073912 (2009).
[7] C. Raufast, A. Tamion, E. Bernstein, V. Dupuis, T. Fournier, T. Crozes, E. Bonet, and W. Wernsdorfer, IEEE Trans. Magn. **44**, 2812 (2008).
[8] L. Thomas, M. Hayashi, X. Jiang, R. Moriya, C. Rettner, and S. S. P. Parkin, Nature (London) **443**, 197 (2006).
[9] G. Bertotti, C. Serpico, and I. D. Mayergoyz, Phys. Rev. Lett. **86**, 724 (2001).
[10] L. Cai and E. M. Chudnovsky, Phys. Rev. B **82**, 104429 (2010).
[11] L. Cai, D. A. Garanin, and E. M. Chudnovsky, Phys. Rev. B **87**, 024418 (2013).
[12] Z. Z. Sun and X. R. Wang, Phys. Rev. B **74**, 132401 (2006).
[13] G. Bertotti, I. D. Mayergoyz, C. Serpico, M. d'Aquino, and R. Bonin, J. Appl. Phys. **105**, 07B712 (2009).
[14] K. Rivkin, N. Tabat, and S. Foss-Schroeder, Appl. Phys. Lett. **92**, 153104 (2008).
[15] Z. Z. Sun and X. R. Wang, Phys. Rev. Lett. **97**, 077205 (2006).
[16] K. Rivkin and J. B. Ketterson, Appl. Phys. Lett. **89**, 252507 (2006).
[17] S. Okamoto, N. Kikuchi, and O. Kitakami, Appl. Phys. Lett. **93**, 142501 (2008).
[18] N. Barros, M. Rassam, H. Jirari, and H. Kachkachi, Phys. Rev. B **83**, 144418 (2011).

[19] S. Okamoto, M. Igarashi, N. Kikuchi, and O. Kitakami, J. Appl. Phys. **107**, 123914 (2010).
[20] X. Wang and P. Ryan, J. Appl. Phys. **108**, 083913 (2010).
[21] We used a transverse Mercator projection defined for $m_y > 0$ by $(X, Y) = -[\arctan(m_z/m_y), \operatorname{atanh}(m_x)]$ and analytically continued for $m_y \leq 0$.
[22] L. F. Alvarez, O. Pla, and O. Chubykalo, Phys. Rev. B **61**, 11613 (2000).
[23] W. Wernsdorfer, E. Orozco, K. Hasselbach, A. Benoit, B. Barbara, N. Demoncy, A. Loiseau, H. Pascard, and D. Mailly, Phys. Rev. Lett. **78**, 1791 (1997).
[24] Please see the Supplemental Material at http://link.aps.org/supplemental/10.1103/PhysRevLett.112.117203 for additional data and numerical simulations of microwave-assisted switching for different delays between pump and probe pulse.